*Optica Applicata, Vol. XLIV, No. 1, 2014*
DOI: 10.5277/oa140114

# Selected nonapeptides in terahertz light

B. Fuglewicz[1], E.F. Pliński[2], P.P. Jarząb[2*], S. Plińska[1],
M. Cebrat[3], K. Nowak[2], L. Augustyn[2], M.J. Walczakowski[5],
M. Mikulics[4], N. Pałka[5], M. Szustakowski[5]

[1]Wrocław Medical University, Wrocław, 50-367, Poland

[2]Wrocław University of Technology, Wrocław, 50-370, Poland

[3]University of Wrocław, Wrocław, 50-383, Poland

[4]Jülich Research Centre, 52425 Jülich, Germany

[5]Military University of Technology, Warsaw, 00-908, Poland

[*]Corresponding author: przemyslaw.jarzab@pwr.edu.pl

Eight synthetic histidine analogues of oxytocin and vasopressin are subject of investigations. The spectra of the peptides have been investigated in the terahertz band. The results are obtained in the terahertz time-domain spectroscopy arrangement.

Keywords: terahertz spectroscopy, peptides, oxytocin, vasopressin, derivatives.

## 1. Introduction

The region of the electromagnetic spectrum has been called far infrared (FIR) in the past, while nowadays it is known as the terahertz band [1–3]. It occupies a region from 10 to 300 $cm^{-1}$. It is necessary to emphasize that usually chemists are interested in the band from 300 to 3000 $cm^{-1}$, roughly saying, where molecular vibrations can be observed (*e.g.*, stretching modes). The terahertz region is a bit different, and interesting rather for physicists and specialists in biomedicine. In this region, intermolecular vibrations can be observed. Moreover, the structure of the investigated molecules can be deduced from the terahertz spectra [4]. The terahertz technique can be helpful to identify unique biologic signatures. The terahertz waves have been used to investigate pharmaceutical compounds [5–8] and amino acids [9–12]. Much larger molecules, as for example peptides, have been investigated as well [12–14]. The terahertz spectroscopy is also a valuable technique to monitor proteins and even DNA structures [15–18]. We have selected the analogues of oxytocin (OT) and vasopressin (VP)

for our terahertz studies. Oxytocin [(Cys-Tyr-Ile-Gln-Asn-Cys)-Pro-Leu-Gly-$NH_2$] and vasopressin [(Cys-Tyr-Phe-Gln-Asn-Cys)-Pro-Arg-Gly-$NH_2$] are peptide hormones, playing an important role in the human body. Impaired secretion of these hormones leads to serious illnesses. Therefore, the analogues of these peptides are developed, with increased activity and selectivity, and decreased side effects. Researches on the development of peptide analogues with the most favorable pharmacological properties typically rely on changes in the amino acid sequence [19]. Such changes affect not only the biological activity of the analogue, but also its physicochemical properties. Involvement of vasopressin and oxytocin in the regulation of human uterine activity is a known effect. OT and VP hormones are intensively investigated using different methods and methodologies. *E.g.*, the structure-activity relationship of the peptide hormone oxytocin is constantly investigated using NMR experiments [20], or can be a target of numerous patents as in the case of vasopressin [21]. Both studied peptides are nonapeptides. The level of the molecule complexity is a challenge for the terahertz technique. Both molecules are very similar. Oxytocin differs from vasopressin only by two amino acids. Isoleucine in the third position is replaced by phenylalanine, and leucine in the eighth position is replaced with arginine in oxytocin and vasopressin chains, respectively.

In our experiment, four analogues of both oxytocin and vasopressin were synthesized. In all derivatives, one of cysteines is exchanged with histidine in the peptide sequence. A carboxyl group (C-terminus) of the selected derivatives was blocked with an amide group, similarly like in native oxytocin and vasopressin hormones, while the amino group (N-terminus) was either left free or blocked with an acetyl group. In that way, altogether eight derivatives have been synthesized and considered in our investigations. The synthesized derivatives differ in some details. In half cases, cysteine and histidine occupy 1st and 6th positions, respectively. In other half cases, the cysteine and histidine are mutually exchanged, as it is shown in Table 1. Other amino acids in both oxytocin and vasopressin are left on their native positions.

The aim of our study is to examine how the changes in the amino acid sequence of the peptide chain affect the spectra of the peptides in the terahertz "finger print" region.

T a b l e 1. Sequences and modifications of investigated peptides.

| Oxytocin analogues | |
|---|---|
| Os17 | Cys-Tyr-Ile-Gln-Asn-His-Pro-Leu-Gly-$NH_2$ |
| Os18 | Ac-Cys-Tyr-Ile-Gln-Asn-His-Pro-Leu-Gly-$NH_2$ |
| Os19 | His-Tyr-Ile-Gln-Asn-Cys-Pro-Leu-Gly-$NH_2$ |
| Os20 | Ac-His-Tyr-Ile-Gln-Asn-Cys-Pro-Leu-Gly-$NH_2$ |
| Vasopressin analogues | |
| Os21 | Cys-Tyr-Phe-Gln-Asn-His-Pro-Arg-Gly-$NH_2$ |
| Os22 | Ac-Cys-Tyr-Phe-Gln-Asn-His-Pro-Arg-Gly-$NH_2$ |
| Os23 | His-Tyr-Phe-Gln-Asn-Cys-Pro-Arg-Gly-$NH_2$ |
| Os24 | Ac-His-Tyr-Phe-Gln-Asn-Cys-Pro-Arg-Gly-$NH_2$ |

## 2. Theoretical assumptions of the experiment

Figure 1 shows schematically a typical arrangement of the terahertz spectrometer working in the system called a terahertz time domain spectroscopy (THz-TDS) [22]. The device works in the same way as any optical interferometer. The most appropriate arrangement is a Mach–Zehnder interferometer, where the beam is carried out with two separated arms and radiation does not pass through the sample twice, as it is in the case of the Michelson interferometer. The difference lies in the fact that some part of one arm beam is converted into terahertz beam (see arms 1 and 2). The signal detection method is the same as in any interferometer. This can be a screen or just an optical detector where the two beams meet together (here: Rx antenna). The measurement system is driven with a laser pulse of a wavelength around 780 nm.

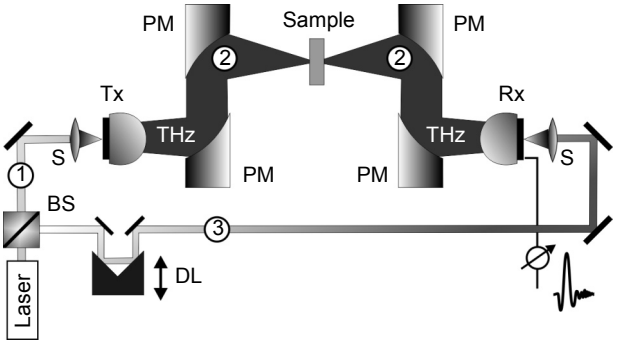


Fig. 1. The arrangement of the terahertz spectrometer; Tx, Rx – terahertz transmitter and receiver, respectively, BS – cubic beam splitter, S – lens, DL – optical delay line, PM – off-axis parabolic mirror.

Laser pulses have a 100 fs time duration and below and they are generated with the time repetition of approximately 80 MHz. The pulses are split on a cubic beam splitter (BS) and addressed in two arms of the interferometer, respectively 1 and 3. A beam arm 1 – still optical – is focused with a microscopic lens (S) at the semiconductor material with a miniature dipole antenna (Tx) with a length of about 100–200 μm technologically imposed at the surface of the LT-GaAs used as a semiconductor. A semiconductor material is usually a specially prepared gallium arsenide plate. Due to a short duration time of the pulse so produced, its spectrum can be in the terahertz range. Starting from Tx antenna, the arm 2 is called THz one, but it is an extension of the arm 1. Still we have two arms of the interferometer: the arms 1 + 2 and the arm 3.

If we insert on the path 2 (see Fig. 1) the test material, it will leave absorption lines in the spectrum of the pulse with the distribution characteristic for the investigated medium. Mathematically, in the Rx antenna receiving signals we measure there is a convolution of two functions – terahertz $E_{\mathrm{ref}}^{\mathrm{THz}}$ and optical $E_{\mathrm{prob}}$ signals – without a sample, as a reference signal. It is known that the conversion of such signals from a time domain to a frequency domain shows that convolution functions can be reduced to their ordinary multiplication what makes the calculation easier.

The signals are recalculated using the Fourier transform, which converts the pulses in the time domain to the frequency domain. They can be expressed as:

$$E_{\mathrm{ref}}^{\mathrm{THz}}(\omega) = E_0^{\mathrm{ref}}(\omega)\exp(-j\varphi_{\mathrm{ref}}) \tag{1}$$

and

$$E_{\mathrm{med}}^{\mathrm{THz}}(\omega) = E_0^{\mathrm{med}}(\omega)\exp(-j\varphi_{\mathrm{med}}) \tag{2}$$

where $E_0^{\mathrm{ref}}$ and $E_0^{\mathrm{med}}$ are the amplitudes of the reference signal and the signal with the sample medium, respectively, $\varphi_{\mathrm{ref}}$ and $\varphi_{\mathrm{med}}$ are the phases of the reference signal and the signal with the sample medium, respectively.

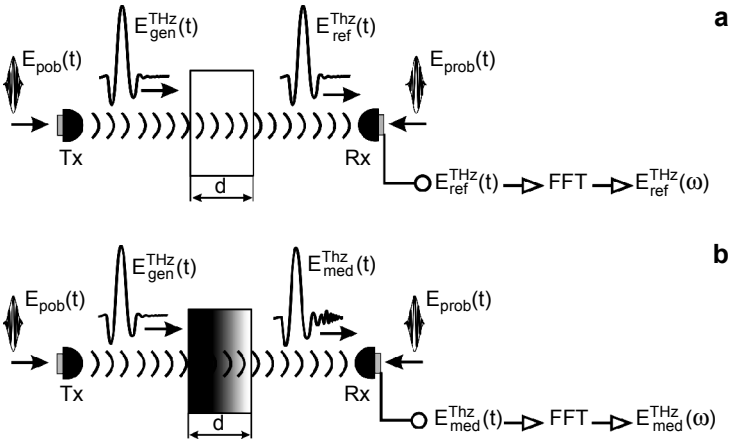


Fig. 2. Coherent homodyne detection – the measuring and calculations of (**a**) the reference signal (without the sample), where $d$ – a space for the sample and (**b**) the signal with the sample, where $d$ – thickness of the sample. FFT – fast Fourier transform operation on the measured signal.

Figure 2 explains schematically the measuring and calculation methods. In Fig. 2**a**, an exciting pulse $E_{\mathrm{pob}}(t)$ creates a terahertz signal in the Tx antenna. In the setup without a sample, the signal $E_{\mathrm{gen}}^{\mathrm{THz}}(t)$ is treated as a reference signal $E_{\mathrm{ref}}^{\mathrm{THz}}(t)$. The same optical exciting signal $E_{\mathrm{pob}}$ is taken as a probing signal $E_{\mathrm{prob}}$, when it is delivered to the receiving antenna Rx. Signals $E_{\mathrm{ref}}^{\mathrm{THz}}(t)$ and $E_{\mathrm{prob}}$ meet together at the receiving antenna Rx, where a homodyne detection is realized. After that, the obtained signal is recalculated into a frequency domain using fast Fourier transform (FFT) $E_{\mathrm{ref}}^{\mathrm{THz}}(t) \rightarrow E_{\mathrm{ref}}^{\mathrm{THz}}(\omega)$. The same procedure is carried out on the setup with the sample medium of $d$ thick. The obtained signal $E_{\mathrm{med}}^{\mathrm{THz}}$ is transformed into a frequency domain $E_{\mathrm{med}}^{\mathrm{THz}}(t) \rightarrow E_{\mathrm{med}}^{\mathrm{THz}}(\omega)$.

After the deconvolution operation we have:

$$\frac{E_{\mathrm{med}}^{\mathrm{THz}}(\omega)}{E_{\mathrm{ref}}^{\mathrm{THz}}(\omega)} = \frac{E_0^{\mathrm{med}}(\omega)}{E_0^{\mathrm{ref}}(\omega)}\exp\left[-j(\varphi_{\mathrm{med}} - \varphi_{\mathrm{ref}})\right] \tag{3}$$

The spectrum of the investigated sample is expressed as an absorption coefficient $\alpha$ *versus* frequency $\omega$

$$\alpha(\omega) \approx -\frac{2}{d} \ln\left(\frac{E_{\text{med}}^{\text{THz}}(\omega)}{E_{\text{ref}}^{\text{THz}}(\omega)}\right) \tag{4}$$

## 3. Measurements

The samples were synthesized at the University of Wrocław, Poland. Samples in a lyophilized powder form were measured in a spacer designed for this purpose. The 300 μm thick spacer is shown in Fig. 3. Two plastic rings each 150 μm thick and with a 4 mm hole inside visible in the centre of the figure created the measurement space. The rings and a sample were fixed between polyethylene (PE) stoppers and pressed with the threaded metal cylinders (Fig. 3). Polyethylene was used as it is transparent for the terahertz radiation [23, 24]. The spacer allows using a small amount of the investigated material – around 1 mg.

Plastics rings used for the apparatus were made of floppy diskettes. As it is known, it contains a large amount of iron particles, and it is not transparent for the terahertz radiation.

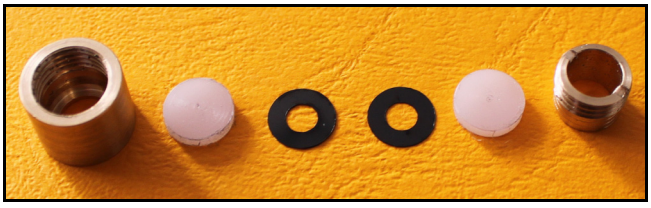

Fig. 3. An assembly picture of the spacer used in the experiment. From the left: a threaded cylinder (left – female, right – male), two polyethylene stoppers, and two plastic rings keeping the 300 μm thick and 4 mm in a diameter room.

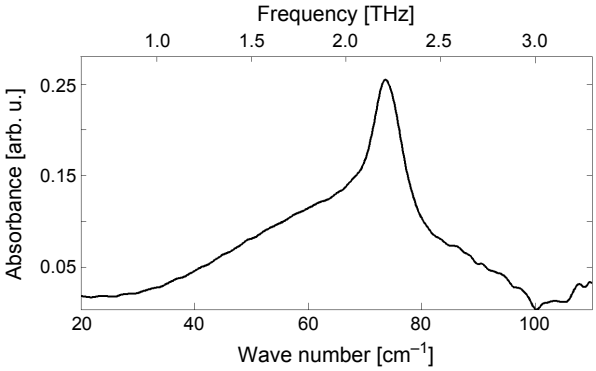


Fig. 4. A spectrum of a polyethylene plate in the terahertz range.

Polyethylene is commonly used in THz system components, but then the measured absorbance data are limited to a narrow spectral range, below 67 $cm^{-1}$ [25]. It was confirmed by our results. Figure 4 shows the absorbance of two 2 mm thick PE plates used in our experiment. As it is seen, the characteristic shows a strong absorption peak around 75 $cm^{-1}$. To avoid the influence of the PE effect on a shape of the measured spectrum, the process of the deconvolution was used in the computational procedure – see Eq. (3). Measurements were performed with the spacer equipped with PE stoppers without the sample to obtain the reference signal $E_{\mathrm{ref}}^{\mathrm{THz}}$, and next with the same stopper filled with the investigated material to get a measured signal $E_{\mathrm{med}}^{\mathrm{THz}}$. The spectrum of the investigated material was obtained according to Eq. (4). In that way, the influence of the PE on the investigated material was eliminated.

## 4. Results and discussion

Table 1 shows the sequences of the eight peptides used in the experiment. Some similarities and differences can be recognized in the structure of investigated peptides. Os17 and Os18 analogues of oxytocin have the same amino acid sequences, but they differ in the N-terminus only. In the case of Os17, the end is free, and in the case of Os18, it is blocked with an acetyl group. In this pair, the cysteine and histidine occupy positions 1st and 6th, respectively.

In the Os19 and Os20 pair, the cysteine and histidine are mutually exchanged. And, like in the previous configuration, the Os20 N-terminus was blocked with an acetyl group.

Analogues of vasopressin are different from oxytocin analogues by the fact that isoleucine in the third position was replaced by phenylalanine, and leucine in the eighth position was replaced with arginine.

As in the case of Os18 and Os20, in the Os22 and Os24 peptide N-termini were blocked with an acetyl group.

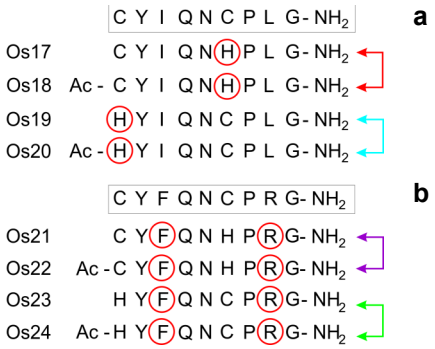


Fig. 5. Diagram of the investigated molecules. Amino acid sequences of the nonapeptides: C – cysteine, Y – tyrosine, I – isoleucine, Q – glutamine, N – asparagine, H – histidine, P – proline, L – leucine, G – glycine, Ac – acetyl, F – phenyloalanine, R – arginine; **a** and **b** figuratively illustrated methodology of the measurements.

The selection of peptides as shown above allows estimating the influence of the blocking of the peptide N-terminus with an acetyl group. The selection of the peptide pairs is illustrated in Fig. 5.

The Os17 and Os18 are comparable (Fig. 6**a**). As it is seen, the absorbance of the both peptides increases monotonically with a wave number. The absorbance for Os18 is slightly higher.

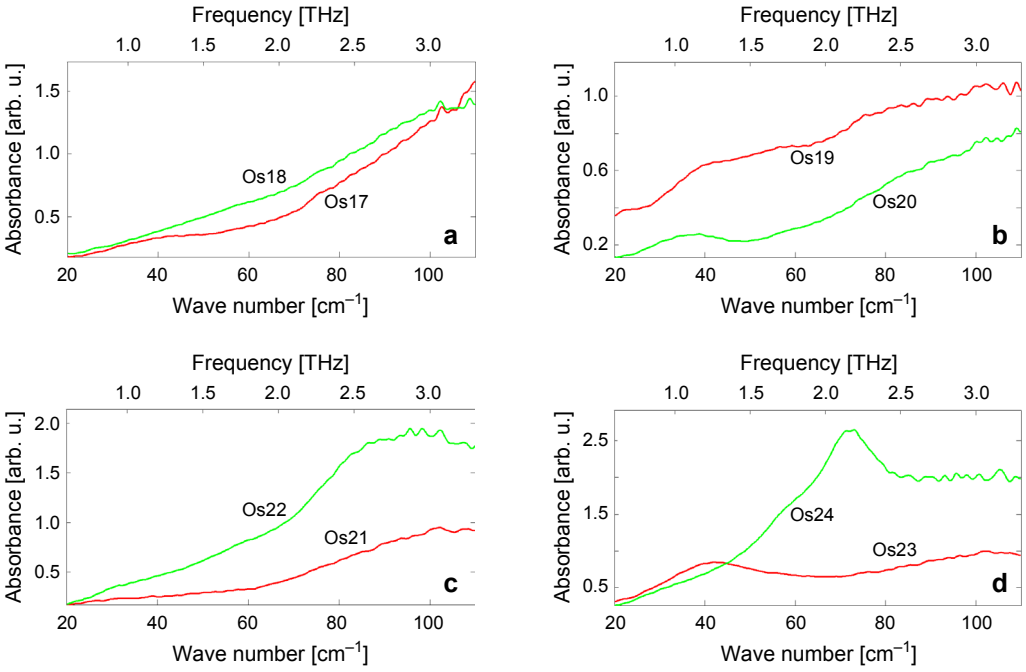


Fig. 6. Terahertz spectra of pairs of Os17–Os18 (**a**), Os19–Os20 (**b**), Os21–Os22 (**c**) and Os23–Os24 (**d**) peptides.

In the case of Os19 and Os20 (Fig. 6**b**), the observed differences are significant. Contrary to the previous pair, Os19 peptide with a free N-terminus shows higher values of absorbance in the whole investigated frequency region. In addition, the absorbance characteristic of Os19 is practically flat in the region of 80–100 $cm^{-1}$, while for Os20 it slightly increases. A 39.0 $cm^{-1}$ absorption line is recognized for Os19, and 38.0 $cm^{-1}$ absorption line is recognized for Os20.

In the case of vasopressin analogues, the differences in absorbance are significantly high – see Figs. 6**c** and 6**d** for Os21–Os22 and Os22–Os23 pairs, respectively. For both pairs, peptides with N-termini blocked by an acetyl group show a higher absorbance, it means, for Os22 and Os24 peptides. Characteristics for Os21 and Os22 do not show spectral details, like Os17 and Os 18. The smooth bands are the result of the lack of the long-range order in the samples. It is typical of amorphous media, what is expected here [26].

As it is seen, Os23 and Os24 absorbance characteristics are practically the same to approximatelly 45.0 $cm^{-1}$. Above this value, the dramatic increase in the absorbance for Os24 is observed, while the absorbance characteristic for Os23 remains almost flat. The Os23 spectrum shows 41.8 $cm^{-1}$, while a 72.0 $cm^{-1}$ strong peak is observed for Os24 peptide.

In the case of Os19, and Os23 and peptides, where the amino group (N-terminus) was left free, and in the case of Os20, Os24 ones with N-terminus blocked with an acetyl group, histidine was placed at the first place, and (as it is seen in Figs. 6**b** and 6**d**) four absorption peaks are easy recognized: Os19 – 39.0 $cm^{-1}$, Os23 – 41.8 $cm^{-1}$, Os20 – 38.0 $cm^{-1}$, and Os24 – 72.0 $cm^{-1}$.

Definitive assignment of the observed modes is difficult because of the lack of reliable algorithms (suitable for simulations of lattice dynamics), which are able to recognize frequencies originated from intermolecular vibrations [8].

Observed spectra in our experiment are likely due to intermolecular modes of the lattice or hydrogen bonds. But it is difficult to estimate whether they are due to hydrogen bond stretching or bending, or bond torsion, or skeletal deformations [27].

In the paper [28] some number of amino acids has been investigated. Vibrational modes below 220 $cm^{-1}$ are shown, and their interpretation is given. They are considered as the hydrogen bond modes, while modes above 220 $cm^{-1}$ up to 650 $cm^{-1}$ are assigned to collective vibrations as: $COO^-$ vibrations (220–270 $cm^{-1}$), $CC^{\alpha}N$ deformations (270–380 $cm^{-1}$), $NH_3^+$ modes (380–480 $cm^{-1}$), $COO^-$ rock/bend/wag vibrations (480–650 $cm^{-1}$). Similarly in the papers [7, 17, 29] hydrogen bonds are responsible for modes below 100 $cm^{-1}$.

Spectra of investigated peptides can be also analyzed for other compositions of peptide pairs. For the next analysis Os17–Os19, Os18–Os20, Os21–Os23, Os22–Os24 pairs are selected. Locations of cysteine and histidine are exchanged mutually in the pairs. Figure 7 illustrates the idea.

For the three investigated pairs (Os17–Os19, Os21–Os23, Os22–Os24 – see Figs. 8**a**, 8**b**, and 8**c**, respectively) higher absorbance is observed for those peptides where histidine occupies the first position in the amino-acid sequence, and cysteine

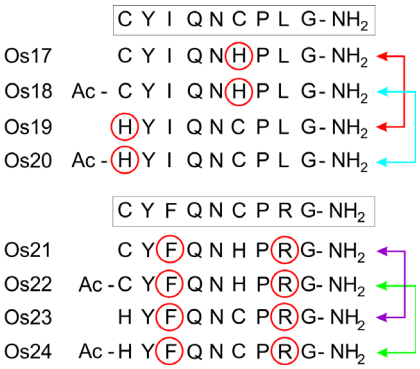


Fig. 7. The Os17–Os19, Os18–Os20, Os21–Os23, Os22–Os24 pairs selected for analysis.

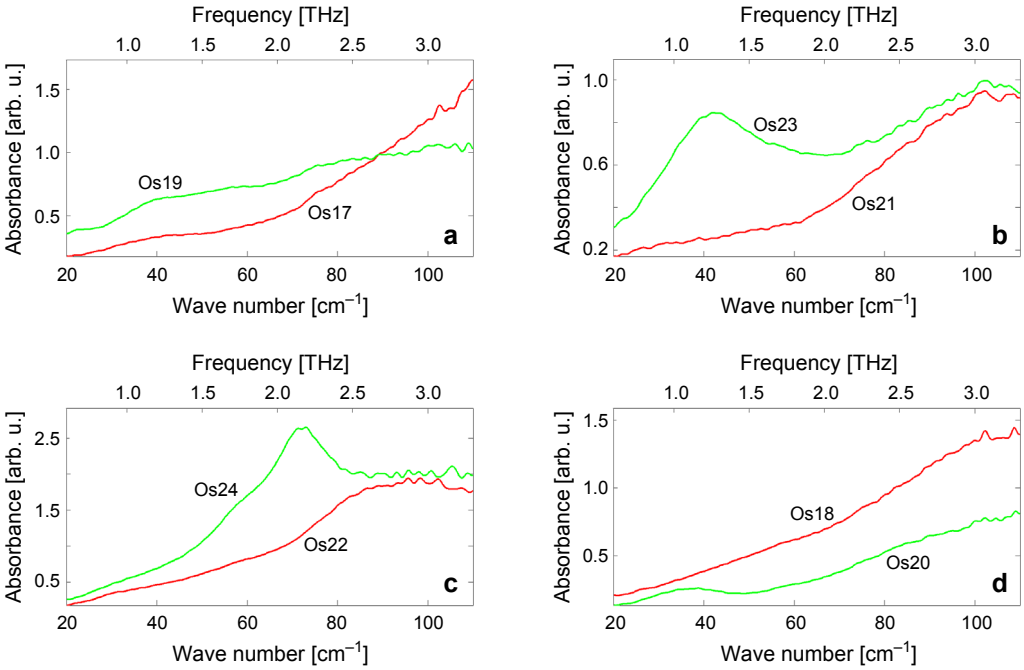


Fig. 8. Terahertz absorbance spectra of the pairs of Os17–Os19 (**a**), Os21–Os23 (**b**), Os22–Os24 (**c**) and Os18–Os20 (**d**) peptides.

the sixth position. This property does not depend on the state of the N-terminus – whether it is blocked or not.

For the Os18–Os20 pair (see Fig. 8**d**) higher absorbance is observed for the peptide with the cysteine occupying the first position of the amino-acid sequence, and histidine the sixth position. But in this case, the N-termini are blocked with an acetyl group for both peptides.

Another possibility is to compare the spectra of oxytocin analogues to the corresponding spectra of vasopressin analogues, as it is shown in Fig. 9.

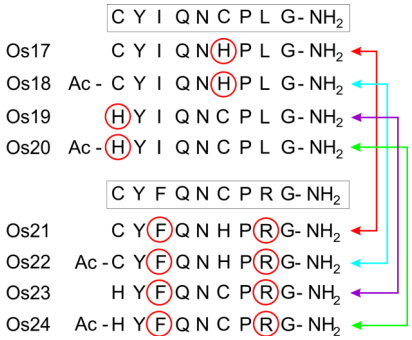


Fig. 9. The Os17–Os21, Os18–Os22, Os19–Os23, Os20–Os24 pairs selected for analysis.

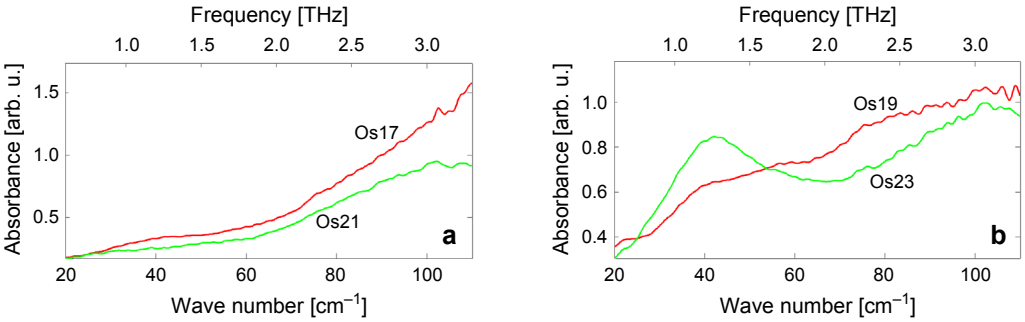


Fig. 10. Terahertz absorbance spectra of the pairs of Os17–Os21 (**a**), and Os19–Os23 (**b**) peptides.

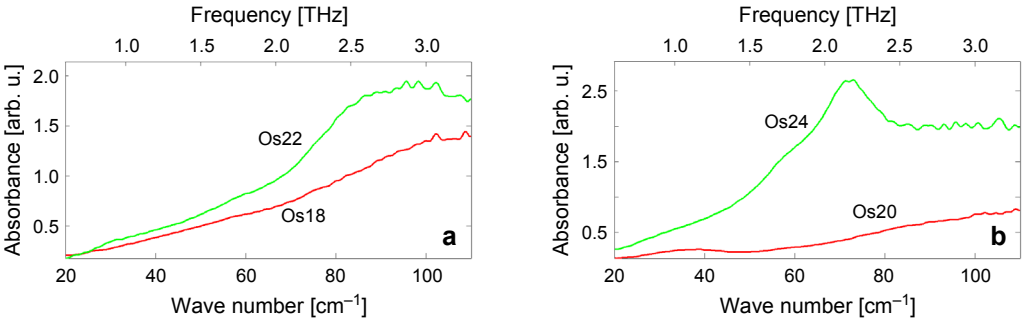


Fig. 11. Terahertz absorbance spectra of the pairs of Os18–Os22 (**a**), and Os20–Os24 (**b**) peptides.

Figure 10**a** demonstrates spectra of both Os17 and Os21 oxytocin derivatives. The peptides have free N-termini and the cysteine appears at the first position of the sequence (see Fig. 9).

Similarly, Fig. 10**b** demonstrates spectra of both Os19 and Os23, but in this case, the first position of the peptides is occupied by histidine (see Fig. 9); oxytocin spectra (Os17 and Os19) have higher value of absorbance in the frequency band. In the case of Os19 and Os23 pair, the Os23 peptide has higher absorbance values than Os19 in the range to 53.0 cm$^{-1}$. An absorption line is observed at 41.8 cm$^{-1}$ for Os23.

A different picture is observed for Os18 and Os22 pair and for Os20 and Os24 one – see Fig. 11.

Spectra of vasopressin analogues Os22 and Os24, see Figures 11**a** and 11**b**, respectively, have higher values of absorbance than oxytocin analogues Os18 and Os20 in all observed frequency ranges. It can be an evidence that the exchange of isoleucine (at the third position of the chain) with phenyloalanine, and the exchange of leucine (at the eight position of the peptide chain) with arginine have little effect on the values of absorbance of the investigated peptides. Decisive influence on the increase in absorbance of investigated peptides is the presence of the acetyl group block-

ing the N-terminus. Location of histidine at the first position of the peptide chain significantly influences the increase in absorbance as well.

## 5. Conclusions

Four analogues of oxytocin and four of vasopressin have been measured using the THz-TDS arrangement. The investigated derivatives differ in the amino acids sequences. We have received eight spectra of the individual oligopeptides. Twin peptides were compared (Os17–Os18, Os19–Os20, Os21–Os22, Os23–Os24), which differ by the fact that one of them had the free N-terminus, and the other was blocked with an acetyl group. We have found that the presence of the acetyl group generally results in an increased absorbance. Peptides were compared, where the cysteine and histidine changed places (Os17–Os19, Os18–Os20, Os21–Os23, Os22–Os24). It was found that the presence of histidine in the first position in the sequence also results in an increased absorbance. We have compared pairs of Os17–Os21 and Os18–Os22 and pairs Os19–Os23 and Os20–Os24, which differ in that isoleucine in the third position was replaced by phenylalanine, and leucine in the eighth position was replaced by arginine. There was no regular effect of such exchange on the level of absorbance of the individual oligopeptides. Four characteristics for Os17, Os18, Os21, and Os22 do not show spectral details. The smooth bands are the result of the lack of the long-range order in the samples. It is typical of amorphous media. Four spectra are characterized by the presence of easy recognized absorption lines with lower wave numbers. They are: Os19 – 39.0 $cm^{-1}$, Os20 – 38 $cm^{-1}$, Os23 – 41.8 $cm^{-1}$, and Os24 – 72.0 $cm^{-1}$. Contemporary methods of computational chemistry do not allow assigning observed terahertz frequencies to suitable modes, contrary to intramolecular vibrations supported by many computational packets. We assign observed in our experiment spectral details to intermolecular modes of the lattice or hydrogen bonds. In our opinion, the terahertz investigations can bring new information about the structure of the peptides.

*Acknowledgements* – The authors would like to thank Justyna Brasuń for very fruitful discussions, and Mikołaj Sułkowski, and Bartosz Suszyński for their assistance.

### References

[1] Mittleman D. [Ed.], *Sensing with Terahertz Radiation*, Springer-Verlag, 2003.
[2] Xi-Cheng Zhang, Jingzhou Xu, *Introduction to THz Wave Photonics*, Springer, 2010.
[3] Sakai K. [Ed.], *Terahertz Optoelectronics*, Springer-Verlag, 2005.
[4] Jiang F.L., Ikeda I., Ogawa Y., Endo Y., *Terahertz absorption spectra of fatty acids and their analogues*, Journal of Oleo Science **60**, 2011, pp. 339–343.
[5] Laman N., Sree Harsha S., Grischkowsky D., *Narrow-line waveguide terahertz time-domain spectroscopy of aspirin and aspirin precursors*, Applied Spectroscopy **62**(3), 2008, pp. 319–326.

[6] YAO-CHUN SHEN, *Terahertz pulsed spectroscopy and imaging for pharmaceutical applications: a review*, International Journal of Pharmaceutics **417**(1–2), 2011, pp. 48–60.
[7] STRACHAN C.J., RADES T., NEWNHAM D.A., GORDON K.C., PEPPER M., TADAY P.F., *Using terahertz pulsed spectroscopy to study crystallinity of pharmaceutical materials*, Chemical Physics Letters **390**(1–3), 2004, pp. 20–24.
[8] ZEITLER J.A., TADAY P.F., NEWNHAM D.A., PEPPER M., GORDON K.C., RADES T., *Terahertz pulsed spectroscopy and imaging in the pharmaceutical settings – a review*, Journal of Pharmacy and Pharmacology **59**(2), 2007, pp. 209–223.
[9] KORTER T.M., BALU R., CAMPBELL M.B., BEARD M.C., GREGURICK S.K., HEILWEIL E.J., *Terahertz spectroscopy of solid serine and cysteine*, Chemical Physics Letters **418**(1–3), 2006, pp. 65–70.
[10] NISHIZAWA J., SASAKI T., TANNO T., *Coherent terahertz-wave generation from semiconductors and its applications in biological sciences*, Journal of Physics and Chemistry of Solids **69**(2–3), 2008, pp. 693–701.
[11] TRUE A.B., SCHROECK K., FRENCH T.A., SCHMUTTENMAER C.A., *Terahertz spectroscopy of histidine enantiomers and polymorphs*, Journal of Infrared, Millimeter and Terahertz Waves **32**(5), 2011, pp. 691–698.
[12] KUTTERUF M.R., BROWN C.M., IWAKI L.K., CAMPBELL M.B., KORTER T.M., HEILWEIL E.J., *Terahertz spectroscopy of short-chain polypeptides*, Chemical Physics Letters **375**(3–4), 2003, pp. 337–343.
[13] BORN B., WEINGÄRTNER H., BRÜNDERMANN E., HAVENITH M., *Solvation dynamics of model peptides probed by terahertz spectroscopy. Observation of the onset of collective network motions*, Journal of the American Chemical Society **131**(10), 2009, pp. 3752–3755.
[14] TAO DING, RUOYU LI, ZEITLER J.A., HUBER T.L., GLADDEN L.F., MIDDELBERG A.P.J., FALCONER R.J., *Terahertz and far infrared Spectroscopy of alanine-rich peptides having variable ellipticity*, Optics Express **18**(26), 2010, pp. 27431–27444.
[15] EBBINGHAUS S., SEUNG JOONG KIM, HEYDEN M., XIN YU, GRUEBELE M., LEITNER D.M., HAVENITH M., *Protein sequence- and pH-dependent hydration probed by terahertz spectroscopy*, Journal of the American Chemical Society **130**(8), 2008, pp. 2374–2375.
[16] GLOBUS T., WOOLARD D., CROWE T.W., KHROMOVA T., GELMONT B., HESLER J., *Terahertz Fourier transform characterization of biological materials in a liquid phase*, Journal of Physics D: Applied Physics **39**(15), 2006, pp. 3405–3413.
[17] BRANDT N.N., CHIKISHEV A.YU., KARGOVSKY A.V., NAZAROV M.M., PARASHCHUK O.D., SAPOZHNIKOV D.A., SMIRNOVA I.N., SHKURINOV A.P., SUMBATYAN N.V., *Terahertz time-domain and Raman spectroscopy of the sulfur-containing peptide dimers: Low-frequency markers of disulfide bridges*, Vibrational Spectroscopy **47**(1), 2008, pp. 53–58.
[18] KAWAGUCHI S., KAMBARA O., PONSECA JR. C.S., SHIBATA M., KANDORI H., TOMINAGA K., *Low-frequency dynamics of biological molecules studied by terahertz time-domain spectroscopy*, Spectroscopy **24**(1–2), 2010, pp. 153–158.
[19] SIEMION I.Z., CEBRAT M., WIECZOREK Z., *Cyclolinopeptides and their analogs – a new family of peptide immunosuppressants affecting the calcineurin system*, Archivum Immunologiae et Therapia Experimentalis **47**, 1999, pp. 143–153.
[20] WITTELSBERGER A., PATINY L., SLANINOVA J., BARBERIS C., MUTTER M., *Introduction of a* cis*-prolyl mimic in position 7 of the peptide hormone oxytocin does not result in antagonistic activity*, Journal of Medicinal Chemistry **48**(21), 2005, pp. 6553–6562.
[21] WISNIEWSKI K., SCHTEINGART C., LAPORTE R., GALYEAN R.F., RIVIERE P., *Peptidics Vasopressin Receptor Agonists*, USA Patent, No. US 2009/0054309 A1.
[22] DEXHEIMER S.L., *Terahertz Spectroscopy: Principles and Applications*, CRC Press, 2008.
[23] KITAGAWA J., OHKUBO T., ONUMA M., KADOYA Y., *THz spectroscopic characterization of biomolecule/water systems by compact sensor chips*, Applied Physics Letters **89**(4), 2006, article 041114.
[24] ZEITLER J.A., KOGERMANN K., RANTANEN J., RADES T., TADAY P.F., PEPPER M., AALTONEN J., STRACHAN C.J., *Drug hydrate systems and dehydration processes studied by terahertz pulsed spectroscopy*, International Journal of Pharmaceutics **334**(1–2), 2007, pp. 78–84.

[25] FLANDERS B.N., CHEVILLE R.A., GRISCHKOWSKY D., SCHERER N.F., *Pulsed terahertz transmission spectroscopy of liquid $CHCl_3$, $CCl_4$, and their mixtures*, Journal of Physical Chemistry **100**(29), 1996, pp. 11824–11835.
[26] WALTHER M., FISHER B.M., UHD JEPSEN P., *Noncovalent intermolecular forces in polycrystalline and amorphous saccharides in the far infrared*, Chemical Physics **288**(2–3), 2003, pp. 261–268.
[27] SHEN S.C., SANTO L., GENZEL L., *THz spectra for some bio-molecules*, Journal of Infrared, Millimeter, and Terahertz Waves **28**(8), 2007, pp. 595–610.
[28] MATEI A., DRICHKO N., GOMPF B., DRESSEL M., *Far-infrared spectra of amino acids*, Chemical Physics **316**(1–3), 2005, pp. 61–71.
[29] BUONTEMPO U., CARERI G., FASELLA P., FERRARO A., *Far-infrared spectra of some globular proteins*, Biopolymers **10**(12), 1971, pp. 2377–2386.

*Received April 26, 2013*
*in revised form August 7, 2013*